
# A literature review and interpretation of the properties of high-$TiO_2$ slags

**H. Kotzé**[1]

**Affiliation:**
[1]Consensi Consulting, Mtunzini, South Africa.

**Correspondence to:**
H. Kotze

**Email:**
hanlie.k@consensi.co.za

**Dates:**
Received: 23 Aug. 2019
Revised: 24 Jan. 2020
Accepted: 13 Feb. 2020
Published: February 2020

**How to cite:**
Kotzé, H.
A literature review and interpretation of the properties of high-$TiO_2$ slags.
The Southern African Insitute of Mining and Metallurgy

DOI ID:
http://dx.doi.org/10.17159/2411-9717/894/2020

ORCiD ID:
H. Kotzé
https://orcid.org/0000-0002-8937-7511

This paper was first presented at *The Eleventh International Heavy Minerals Conference*, 5–6 August 2019, The Vineyard, Cape Town, South Africa.

**Synopsis**

**The properties of high-$TiO_2$ slags are markedly different from those of many other metallurgical slags. The objective of this paper is twofold: firstly, to assemble in one document the $TiO_2$ slag properties, including $Ti^{3+}/Ti^{4+}$ ratio, liquidus temperatures, heat capacity, density, viscosity, thermal conductivity, and electrical conductivity: all expressed in terms of temperature and composition dependency. Secondly, this paper attempts to correlate published experimentally measured data with theoretically based parameters, which will enable the application of the measured properties to wider slag compositions within the pseudobrookite-$TiO_2$ slag system.**

**Keywords**
**high-$TiO_2$ slag, properties.**

## Introduction

Slag properties are an essential tool in problem solving, both in equipment design and metallurgical process control. Experimental work on high-$TiO_2$ slags is particularly difficult because of their chemically corrosive nature and compositional sensitivity to oxygen partial pressure. While ample publications are available and are still being produced for silicate-based slags, comparatively few results are available for high-$TiO_2$ slags. The objective of this work is firstly to summarize the essential properties for liquid $TiO_2$ slags. Secondly, an attempt is made to derive correlations from the published experimental work which are based on a theoretical concept. In this way, it is believed that the experimental data can be cautiously extrapolated to other high-$TiO_2$ slags. To this end, a set of typical high-$TiO_2$ slags based on a data-set published in earlier work (Kotze and Pistorius, 2010) is used throughout this paper. The chemical composition of this set is given in Table I. Although 94%$TiO_2$ is not considered 'typical', it was included in the example slags because many producers migrate to higher $TiO_2$ slags.

The experimental data cited in this work is by no means claimed to be all-inclusive. Glimmers of work done in Eastern European countries are present, though not easily interpreted by English-speaking researchers. On occasion experimental data was not used because of a discrepancy in the data or experimental method.

## Slag properties

### *$Ti^{3+}/Ti^{4+}$ ratio*

Titania slag compositions are typically expressed as $TiO_2$ because analytical methods measuring the total titanium are fast and less cumbersome than the wet chemistry titration method required to measure $Ti^{3+}$ (Tranell, Ostrovski, and Jahanshahi, 2002). When appreciable amounts of $Ti_2O_3$ are included in the $TiO_2$ value, titania is expressed as the equivalent $TiO_2$. In these instances, slag assays exceed 100 because the oxygen is overestimated. The assay total is therefore an indication of the level of reduction. Previous attempts by the author to correlate measured $Ti^{3+}$ values with assay totals yielded unsatisfactory results.

The balance between $Ti^{4+}$ and $Ti^{3+}$ follows Reaction [1] and like other transition elements, it is governed by a redox reaction such as the O-type behavior of Reaction [2] (Tranell, Ostrovski, and Jahanshahi, 2002). The $Ti^{3+}/Ti^{4+}$ ratio is therefore expected to be dependent on the oxygen partial pressure and the oxygen activity in the slag bath. Tranell and co-workers (Tranell, Ostrovski, and Jahanshahi, 1997, 2002) investigated these relationships in $TiO_2$-$Ti_2O_3$-$SiO_2$-CaO slags and found the $Ti^{3+}/Ti^{4+}$ ratio to depend on the oxygen partial pressure raised to the power of 0.21 (Tranell, Ostrovski, and Jahanshahi, 1997) and 0.23 (Tranel, Ostrovski, and Jahanshahi, 2002). Using optical basicity to represent oxygen activity, they derived a correlation using temperature, oxygen partial pressure, and optical basicity to calculate the $Ti^{3+}/Ti^{4+}$ ratio. This correlation yielded good results with all the slags they investigated, but not with those of other researchers.

*Table I*

**Compositions of example industrial $TiO_2$ slags based on the data-set given by Kotze and Pistorius, 2010**

| | $TiO_{2\ eq}$ | FeO | $SiO_2$ | $Al_2O_3$ | CaO | MgO | MnO |
|---|---|---|---|---|---|---|---|
| Slag 1 | 94.0 | 4.0 | 1.5 | 1.5 | 0.10 | 1.0 | 2.1 |
| Slag 2 | 91.0 | 7.0 | 1.4 | 1.4 | 0.10 | 1.0 | 2.0 |
| Slag 3 | 88.0 | 10.0 | 1.2 | 1.3 | 0.10 | 1.0 | 1.9 |
| Slag 4 | 85.0 | 13.0 | 1.1 | 1.2 | 0.10 | 0.9 | 1.8 |
| Slag 5 | 82.0 | 16.0 | 0.9 | 1.1 | 0.10 | 0.8 | 1.7 |

$$TiO_2 \Leftrightarrow TiO_{1.5} + {}^1/_4\, O_2 \quad [1]$$

$$TiO_4^{4-} \leftrightarrow Ti^{3+} + {}^7/_2\, O^{2-} + {}^1/_4\, O_2 \quad [2]$$

In this work, electronic polarizability was investigated as an alternative measure to predict the activity of oxygen. Electronic polarizability is described as the 'ability of oxygen to transfer electron density to surrounding cations' (Dimitrov and Komatsu, 2010). It is a measure of the propensity of compounds to donate charge from oxygen ions to the surrounding electron cloud (Duffy and Ingram, 1976). In this context, $Ca^{2+}$ with a cation polarizability of 1.57Å$^3$ is 'generous' while $Si^{4+}$ at 0.284 Å$^3$ is comparatively 'stingy.' A few mutually exclusive data-sets exist to calculate electronic polarizability. The data used in this work is based on the large data-set of dynamic polarizabilities published by Shannon and Fischer (2016) which includes a value for the cation polarizability of $Ti^{3+}$. The $Ti^{3+}/Ti^{4+}$ ratios of the CaO-$SiO_2$-$TiO_x$ slags from Tranell were found to correlate well with the ratio of the polarizabilities of $Ca^{2+}$ and $Si^{2+}$, $R_\alpha = {}^{X_{CaO}\alpha_{Ca2+}}/_{X_{SiO2}\alpha_{Si4+}}$ (polarizability Å$^3$; mole fraction $X$).This result corroborates the polarizability ratio of $Ca^{2+}$ and $Si^{4+}$ as a measure of the oxygen activity in the bath. The $Ti^{3+}/Ti^{4+}$ ratios of the slags Tranell studied were subsequently calculated using a correlation with two parameters: the experimental oxygen partial pressure and the polarizability ratio $R\alpha$. Figure 1 shows the results of this correlation to compare well with the experimental $Ti^{3+}/Ti^{4+}$ ratios.

The validity of the correlation between oxygen partial pressure, electronic polarizability, and Ti valency was tested against industrial $TiO_2$ slags using measurements reported by Geldenhuys and Pistorius (1999). These workers measured the oxygen partial pressure in pilot plant $TiO_2$ slags and reported the $TiO_2$ and $Ti_2O_3$ values of the slags at the time of measurement. Their measured oxygen partial pressures in the slags are plotted as the circles in Figure 2. Since the full assays of the slags used in the Geldenhuys study were not given, their results are compared with the calculated $TiO_2$ and $Ti_2O_3$ values of the example slags in Table I using the correlation derived from the work by Tranell. This is not ideal, but a reasonable replacement, as the impurity levels of the ilmenites used in the Geldenhuys study and those used in the Kotze (Kotze and Pistorius, 2010) study – on which the example slags were based were similar. The calculated results shown with the solid and broken lines in Figure 2 compare well with the experimental data. It is worthwhile to note that several studies found the same $Ti^{3+}/Ti^{4+}$ ratios in industrial slags as were found in the Geldenhuys pilot plant study. Few of these results are published such as the industrial slag data points given in Figures 4 to 6, but many are unpublished due to intellectual property rights.

The dependency of the $Ti^{3+}/Ti^{4+}$ ratio on the oxygen partial pressure and $CaO/SiO_2$ ratio (based on the work by Tranell) is summarized in Figure 3. Lower oxygen partial pressures lead to greater reduction and hence higher $Ti^{3+}/Ti^{4+}$ ratios. Higher $CaO/SiO_2$ ratios create higher oxygen activity, which in turn decreases the $Ti^{3+}/Ti^{4+}$ ratio. In a given smelting process the oxygen partial pressure is largely governed by the Fe FeO equilibrium in the slag (Pistorius, 2007), while the $CaO/SiO_2$ ratio is determined by the raw material quality.

In an earlier paper Tranell also reports MgO to affect the $Ti^{3+}/Ti^{4+}$ ratio (Tranell, Ostrovski, and Jahanshahi, 1997). A correlation including the polarizability of $Mg^{2+}$ did not fit the industrial data. The industrial data was a small set, though, and it does not exclude the potential of MgO (as possibly $Al_2O_3$) to – similarly to CaO and $SiO_2$ influence the $Ti^{3+}/Ti^{4+}$ ratio. Future work will investigate this possibility.

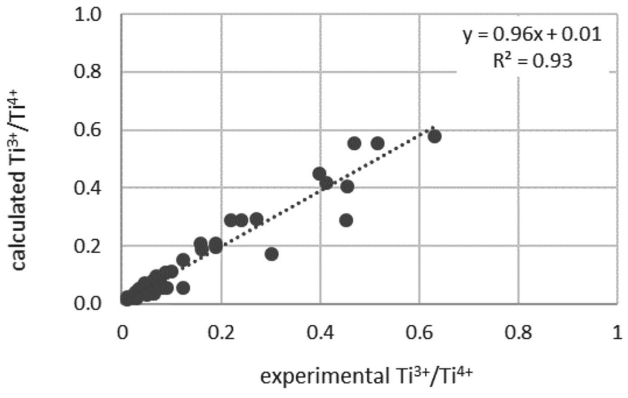


**Figure 1—Comparison of the experimental $Ti^{3+}/Ti^{4+}$ ratios (Tranell, Ostrovski, and Jahanshahi, 2002) against the calculated $Ti^{3+}/Ti^{4+}$ ratio**

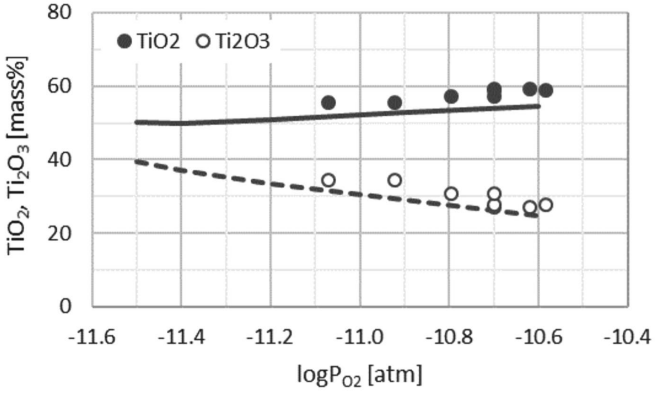


**Figure 2—Measured oxygen partial pressure in $TiO_2$ slags against equivalent $TiO_2$. Circles: pilot plant measurements (Geldenhuis and Pistorius, 1999), line: calculated in this work using the correlation derived from the work of Tranell, Ostrovski, and Jahanshahi (2002)**

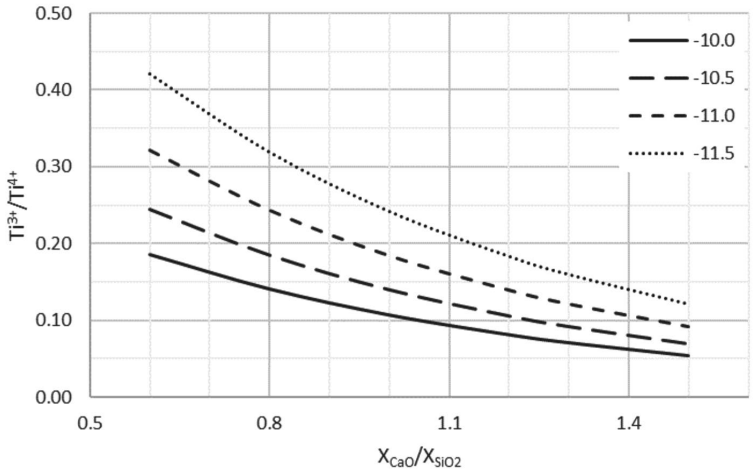


**Figure 3—$Ti^{3+}/Ti^{4+}$ ratios calculated from the oxygen partial pressure (log $Po_2$ [atm] given in the legend) and $CaO/SiO_2$ molar ratio**

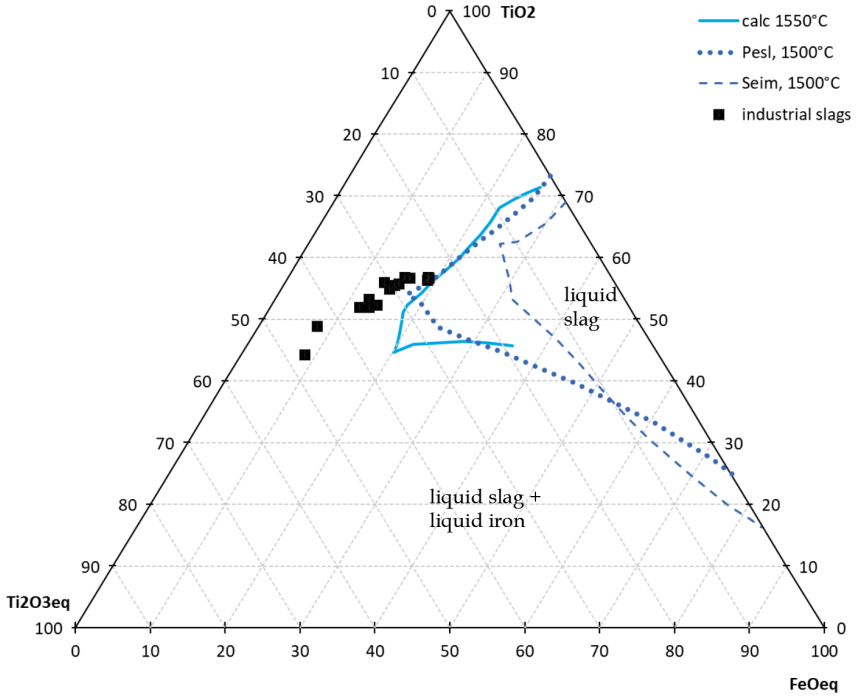


**Figure 4—Liquidus isotherms at 1500°C from Pesl - dotted lines (Pesl and Eric, 1999), and Seim – broken lines (Seim, 2011). The solid line represents the isotherm for 1550°C calculated from the thermodynamic data of Eriksson (Eriksson and Pelton, 1993; Eriksson and Pelton, 1996). Axes are in mass%**

## Liquidus temperatures

Pesl and Eriç (1999) conducted experimental work on slags of the $TiO_2$-$Ti_2O_3$-FeO system, controlling the oxygen partial pressure with CO-$H_2$ gas mixtures, and calibrating slag samples at 1500°C and 1600°C in platinum or molybdenum crucibles for 6 to 8 hours before rapidly quenching them to capture the high-temperature phases. Their predicted liquidus isotherms for 1500°C and 1600°C are reproduced for axes in mass% and given in Figure 4 and Figure 5 as dotted lines. No accuracy or error prediction was reported.

Seim melted slags in an induction furnace with a slag freeze-lining to protect the crucible walls (Seim, 2011; Seim and Kolbensen, 2010). Experiments were conducted in an Ar atmosphere, using titanium metal and haematite additions to control the level of reduction. Liquidus temperatures were determined from cooling curves captured by a spectropyrometer looking down onto the upper surface of the slag. The tolerances for individual measurements on the iron-saturated samples are given as 4.9°C to 33.3°C. Seim modelled a liquidus surface for the $FeTiO_3$-$Ti_2O_3$-$TiO_2$ system using the measured liquidus temperatures of the iron-saturated slags and expanding the thermodynamic data-set with two optimized ternary parameters. The model is considered to accurately predict the measured liquidus temperatures of the iron-saturated slags. The liquidus temperature measurements on the iron-unsaturated samples were unexpectedly and unexplainably lower and not used in the modelling exercise. Despite this, the measured liquidus temperatures of the iron-unsaturated slags plot on average 108°C below the modelled liquidus and 59°C above the modelled solidus temperatures. The model isotherms for 1500°C, 1600°C, and 1700°C were reproduced to have $TiO_2$, $Ti_2O_3$, and FeO as corners of the ternary and are shown in Figure 4, Figure 5, and Figure 6 as broken lines.

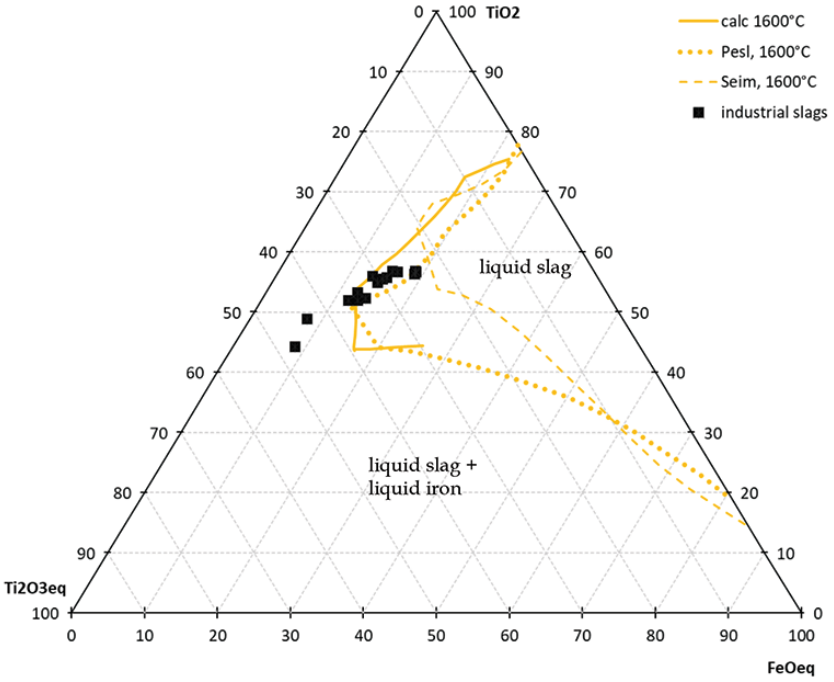


**Figure 5—Liquidus isotherms at 1600°C from Pesl - dotted lines (Pesl and Eric, 1999), and Seim – broken lines (Seim, 2011). The solid line represents the isotherm for 1600°C calculated from the thermodynamic data of Eriksson (Eriksson and Pelton, 1993; Eriksson and Pelton, 1996). Axes are in mass%**

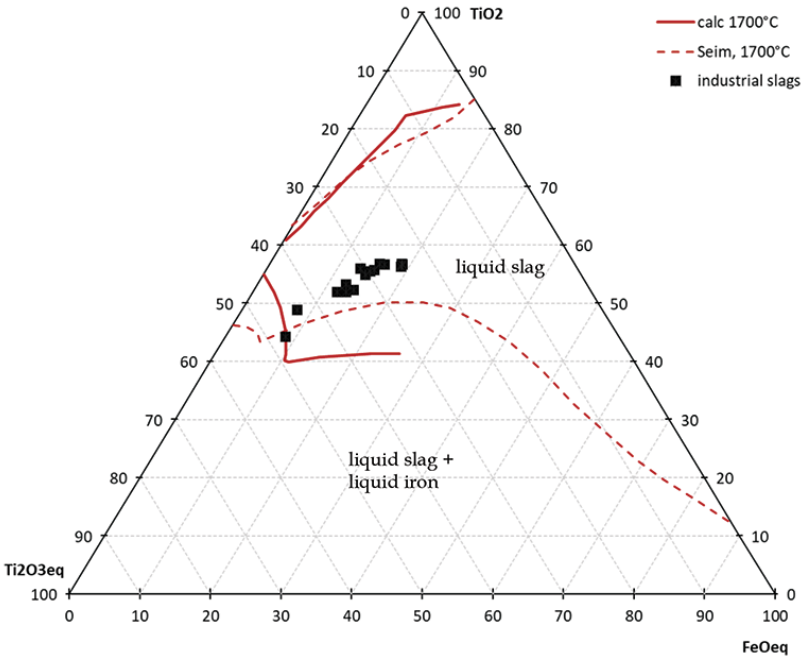


**Figure 6—Liquidus isotherms at 1700°C Seim – broken lines (Seim, 2011). The solid line represents the isotherm for 1700°C calculated from the thermodynamic data of Eriksson (Eriksson and Pelton, 1993; Eriksson and Pelton, 1996). Axes are in mass%**

Thermodynamic data for the binary systems $TiO_2$-FeO and $Ti_2O_3$-$TiO_2$ were published by Eriksson and Pelton (1993) and they illustrated the validity of using this data to calculate the solid phase relationships in the ternary system below 1400°C. They did not publish liquidus predictions (Eriksson and Pelton, 1996). The maximum inaccuracy of the data was given as ±20°C. In the present work the thermodynamic data from Eriksson were used in the Modified Quasichemical Approach (Pelton and Blander, 1986) to calculate the liquidus temperatures in the $TiO_2$-$Ti_2O_3$-FeO system. A temperature, dependent activity coefficient was calculated for the pseudobrookite $M_3O_5$ phase from the experimental data by Pesl (Pesl and Eric, 1999). The calculated liquidus isotherms for 1550°C, 1600°C, and 1700°C are shown Figure 4, Figure 5, and Figure 6 as solid lines. The low-temperature trough these isotherms along approximately 55%$TiO_2$ is in line with the experimentally measured low melting point measured in argon by Brauer and Littke (1960) for the $TiO_2$ $Ti_2O_3$ binary: 1660°C between $TiO_{1.70}$ and $TiO_{1.75}$ (43% to 53% $TiO_2$).

All three isotherm sets show a liquid slag field with (i) an upper phase boundary with the liquid slag + $TiO_x$ phase field, (ii) a lower phase boundary with the liquid slag + liquid iron phase

field, and (iii) a boundary with the liquid slag + $M_3O_5$ + liquid metal phase field. The two upper phase boundaries at 1700°C (*i.e.* the calculated, and Seim prediction) are very similar, and so are the upper phase boundaries of these two sets for 1500°C and 1600°C up to 20%$Ti_2O_3$ – refer to Figure 7. Beyond 20% $Ti_2O_3$ the calculated isotherms predict the liquid slag phase field to extend towards $TiO_2$.$Ti_2O_3$, similar to the dotted 1600°C and 1500°C isotherms by Pesl. The lower boundary separating the liquid slag from the liquid slag + liquid iron phase field, is predicted to lie closer to the $TiO_2$ apex by the Seim model.

To place the liquidus isotherms in Figures 4 to 6 in context with industrial slags, compositions of typical as-tapped $TiO_2$ slags from three different smelters (Pistorius, 2002) are shown as dark squares on the ternaries. For the high-FeO slags the dotted 1500°C and 1600°C upper boundary isotherms by Pesl imply a 100°C drop in liquidus with a ±1% change in FeO (approximately 19% to 18%). This seems an unlikely discontinuity in the known FeO-liquidus temperature relationship of the system. The more likely case is a more gradual temperature gradient as shown by the calculated 50°C spaced isotherms in Figure 7. These are also in agreement with the isotherms by Seim - at least up to 20%$Ti_2O_3$.

According to the calculated isotherms the industrial slag series have liquidus temperatures ranging from 1550°C for 20%$FeO_{eq}$ up to 1700°C for ±9%$FeO_{eq}$, while the broken line isotherms (Seim model) indicate a liquidus range starting somewhere above 1600°C to just over 1700°C. Given the stated tolerances and inaccuracies, the different sets of isotherms are regarded to give similar results, especially in the area of concern for typical industrial $TiO_2$ slags. It will be worthwhile, though, to clarify the discrepancy in the size of the liquid slag phase fields as predicted by the different sets of isotherms.

Figure 7 shows how the liquidus increases with decreasing %FeO: higher reduction yields a higher slag liquidus. However, for a given FeO content, *e.g.* 10mass%, higher reduction will increase the $Ti^{3+}/Ti^{4+}$ ratio, which will decrease the liquidus, until the $Ti^{3+}/Ti^{4+}$ ratio crosses the low liquidus trough between $TiO_2$ and $Ti_2O_3$. On the lower $TiO_2$ and higher $Ti_2O_3$ side of this trough, the liquidus will increase again with increasing $Ti^{3+}/Ti^{4+}$. In practice, where a process receives a stable ilmenite quality, higher reduction will lead to a simultaneous decrease in FeO and an increase in $Ti_2O_3$, and the net effect will be an increase in liquidus, though smaller in size than what would have resulted from a decrease in FeO only.

To apply phase temperature behaviour from the ternary FeO-$TiO_x$ (Figure 7) system to industrial slags, the gangue oxides are grouped into the so-called equivalent FeO and equivalent $Ti_2O_3$ values, calculated with Equations [3] and [4] (percentages as mass%, molecular weight M [g/mol]) (Pistorius, 2007). $FeO_{eq}$ and $Ti_2O_{3\ eq}$ were shown to correlate, following the stoichiometric relationship of the pseudobrookite solid solution $TiO_2$.$(Ti^{3+}Al^{3+}Cr^{3+})_2O_3$ $(Fe^{2+}Mg^{2+}Mn^{2+})O.2TiO_2$, in short referred to as $M_3O_5$. Researchers have shown MgO, MnO, and $Al_2O_3$ to partition to the dominant $M_3O_5$ (pseudobrookite) phase thereby stabilizing this phase (Borowiec, 2009; Pistorius, 2002). There are indications that MnO does not fully partition to the $M_3O_5$ phase but that a potentially significant portion thereof separates to the silicate phase (Seim, 2011; Pesl and Eric, 2002). Without quantitative data on the behaviour of MnO though, the correlation showed by Pistorius is followed. The liquidus isotherms in Figure 7 can therefore applied to industrial slags when the FeO and $Ti_2O_3$ are expressed in their equivalent forms. The $FeO_{eq}$ and $Ti_2O_{3\ eq}$ of the example slags (Table I), together with their calculated liquidus temperatures, are listed in Table II.

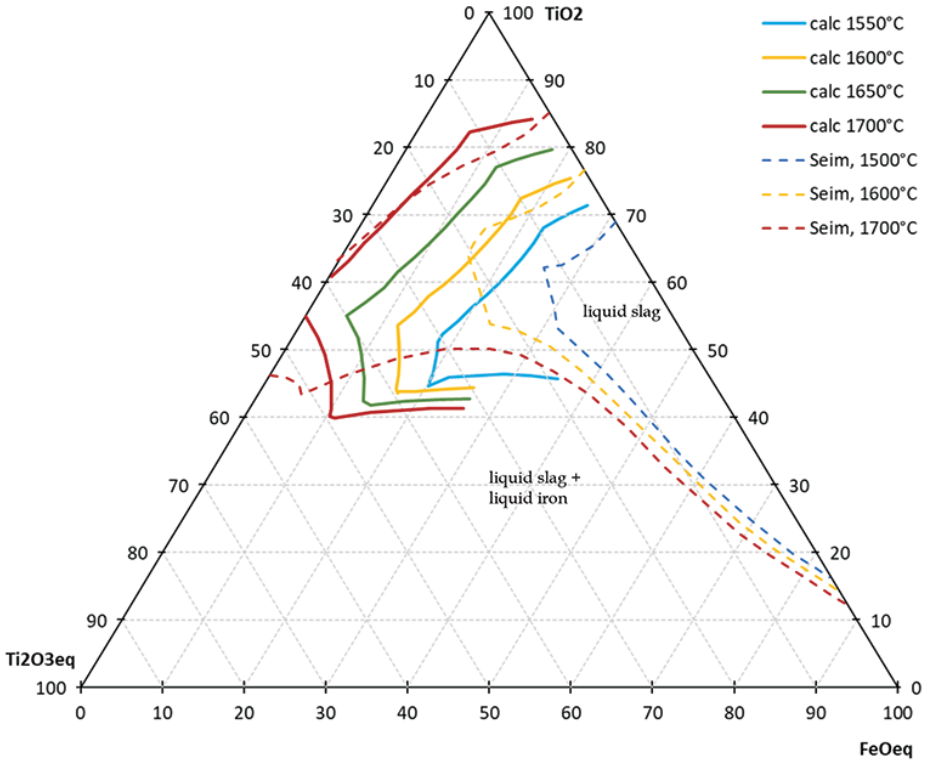


**Figure 7—Calculated liquidus isotherms between 1550°C and 1750°C at 50°C intervals. Axes are in mass%**

*Table II*

**Calculated liquidus temperatures (°C) of the example industrial slags from Table I, using the $FeO_{eq}$ and $Ti_2O_{3\ eq}$ [mass%]**

| | $TiO_{2\ eq}$ | $TiO_2$ | $FeO_{eq}$ | $Ti_2O_{3\ eq}$ | $T_{liquidus}$ |
|---|---|---|---|---|---|
| Slag 1 | 94.0 | 50.1 | 7.9 | 40.9 | 1628 |
| Slag 2 | 91.0 | 49.9 | 10.8 | 38.3 | 1604 |
| Slag 3 | 88.0 | 51.0 | 13.7 | 34.6 | 1588 |
| Slag 4 | 85.0 | 52.8 | 16.4 | 30.2 | 1571 |
| Slag 5 | 82.0 | 54.5 | 19.1 | 25.8 | 1555 |

$$\%FeO_{eq} = \%FeO + \left(\frac{\%MgO}{M_{MgO}} + \frac{\%MnO}{M_{MnO}}\right) M_{FeO} \quad [3]$$

$$\%Ti_2O_{3\ eq} = \%Ti_2O_3 + \left(\frac{\%Cr_2O_3}{M_{Cr2O3}} + \frac{\%V_2O_5}{M_{V2O5}} + \frac{\left(\%Al_2O_3 - \frac{SiO_2}{3}\right)}{M_{Al2O3}}\right) M_{Ti2O3} \quad [4]$$

High-$TiO_2$ slags have a narrow gap between liquidus and solidus temperatures. Seim measured the liquidus and solidus temperatures on synthetic slags using differential thermal analysis/thermal gravity analysis (Seim, 2011). For a $TiO_2$-$Ti_2O_3$-5.6%FeO slag the liquidus and solidus were 1696°C and 1682°C respectively, and for a $TiO_2$-$Ti_2O_3$-16.9%FeO slag, 1664°C and 1644°C respectively. These results imply a narrow temperature gap of 14°C to 20°C between liquidus and solidus. Borowiec (2009) measured solidus and liquidus temperatures on slags with 11–12%, 6–7%, and 2% gangue impurities (the publication gives the impurities for the first and third slag, while impurities for the second slags were deduced from other publications using the same slag). The temperature differences were 136°C, 83°C, and 66°C respectively (Borowiec, 2009). Provided the $SiO_2$ content in the gangue impurities is low (*i.e.* <5% in >10% total gangue, and <3% in <7% total gangue), these differences are indications of the solidus temperatures of high-$TiO_2$ slags.

## Heat capacity

The heat capacities of liquid $TiO_2$ slags were reported by Kotze and Pistorius (2010) and are repeated here, Equation [5] ($C_p$ in J/kg.K). The heat capacity values for the example slags in Table I are listed in Table III.

$$C_p = 0.0561\left(\%FeO_{eq}\right)^2 - 3.3668\left(\%FeO_{eq}\right) + 1044.4 \quad [5]$$

## Density

With most liquid slag systems, a density calculation needs to incorporate the enthalpy of mixing. For slags with only a small deviation from ideality, such as high-$TiO_2$ slags (Eriksson and Pelton, 1993; Gaskell, 2008, p. 247), a weighted average of the densities of the pure liquids suffices. The density of liquid $TiO_2$ was taken as 3.3 g/cm³ at 1600°C from the measurements by Dingwell (1991). The density of liquid $Ti_2O_3$ was measured by Ikemiya *et al.* under an Ar-$H_2$ gas mixture (1993); extrapolated to 1600°C, $Ti_2O_3$ has a density of 4.0 g/cm³. Finally, the density of liquid FeO was taken as 4.4 g/cm³ at 1600°C based on the measurements done by Xin *et al.* (2019). The resultant calculated densities for the example slags (Table I) are given in Figure 8. It is concuded that typical high-$TiO_2$ slags have a density range

*Table III*

**Heat capacities (J/kg.K) of the example slags in Table I, liquid phase**

| Slag 1 | Slag 2 | Slag 3 | Slag 4 | Slag 5 |
|---|---|---|---|---|
| 1021 | 1015 | 1009 | 1004 | 1001 |

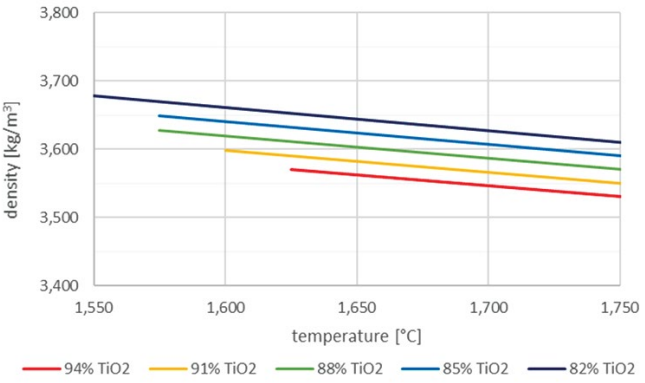


**Figure 8—Calculated densities of the example slags in Table I, liquid state. The legend indicates $TiO_{2\ eq}$.**

of 3.5 g/cm³ to 3.7 g/cm³. This is lower than the temperature-independent value of 3.8 g/cm³ often cited in literature (Kotze and Pistorius, 2010; Zietsman and Pistorius, 2006). Figure 8 shows that the slag densities decrease with increasing temperature, as well as with increasing total $TiO_2$.

## Electrical conductivity

The experimental measurements of the electrical conductivities of $TiO_2$ slags by Desrosiers are reproduced in Figure 9 (Desrosiers, Ajersch, and Grau, August 1980). The electrical conductivity of $TiO_2$ slags is exceptionally high compared to silicate slags, which have conductivities in the order of 0.1 up to less than 10 $\Omega^{-1}$.cm$^{-1}$. High-FeO slags (>70%FeO) have similar and even higher electrical conductivities compared to the titania slags (Jiao and Themelis, 1988; Frederikse and Hosler, 1973). The Desrosiers slags form two distinct groups: those with low gangue (oxides excluding Fe and Ti oxides: 5–6%, 66% to 79%$TiO_{2\ eq}$), and high gangue (15–17% gangue, 80% to 88%$TiO_{2\ eq}$).

Since electrical conductivity is the movement of electron charges, the concept of electronic polarizability was tested against the experimental electrical conductivity measurements. By using the polarizability of the oxide components (Table IV), it was possible to reproduce the electrical conductivities of the high-gangue $TiO_2$ slags using a correlation of the form given in Equation [6] (electrical conductivity $\sigma$ [$\Omega^{-1}$cm$^{-1}$]; electronic polarizability of the slag $\alpha_{slag}$ [Å³] calculated with Equation [7] and the oxide polarizabilities given in Table IV; $a$ a constant; and $n$ a temperature-dependent constant). The calculated electrical conductivities for the high-gangue group (lower $TiO_{2\ eq}$) are given by the broken lines in Figure 9: these calculated values correspond remarkably well with the measured data from Desrosiers.

$$\sigma_{high\ gangue} = a\left(\frac{\alpha_{slag}}{10}\right)^n \quad [6]$$

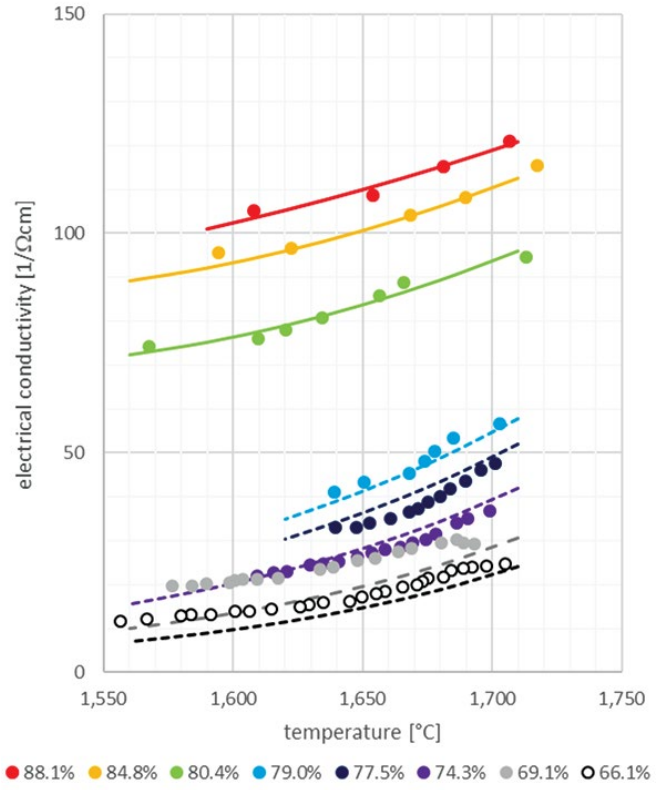


**Figure 9—Electrical conductivities of liquid $TiO_2$ slags. Circles are experimental measurements (Desrosiers, *et al.*, August 1980); lines are calculated values (this work). Broken lines are calculated using Equation [6]; solid lines used Equation [6] combined with [8]. The legend indicates %$TiO_{2\ eq.}$**

*Table IV*

**Electronic polarizabilities of oxides calculated from cation and oxygen anion polarizabilities (Shannon and Fischer, 2016)**

| | $TiO_2$ | $Ti_2O_3$ | FeO | $Al_2O_3$ | CaO | MgO | MnO | $SiO_2$ | $Cr_2O_3$ |
|---|---|---|---|---|---|---|---|---|---|
| $\alpha_i$ (Å$^3$) | 8.590 | 12.570 | 3.830 | 6.306 | 3.360 | 2.441 | 3.864 | 3.864 | 11.410 |

$$\alpha_{slag} = \sum (X_i \alpha_i) \quad [7]$$

$$R_{valency} = (X_{Fe2+} + X_{Ti3+}) \Big/ (X_{Fe2+} + X_{Ti3+} + X_{Ti4+}) \quad [8]$$

Applying Equation [6] to the low-gangue group (high-$TiO_{2\ eq}$) yielded fair, but not, good results. The addition of a temperature-dependent valency ratio $R_{valency}$, Equation [8], improved the calculation significantly: the results are shown by the solid lines in Figure 9.

The electrical conductivities calculated for the example slags (Table I) are shown in Figure 10. The results of the 82%, 85%, and 88%$TiO_{2\ eq}$ slags correspond with the measured values of similar slags shown in Figure 9. The predicted electrical conductivities for the 91% and 95% $TiO_2$ slags cannot be verified against experimental data, but since the calculation is based on parameters which supports the theory of electrical conductivity in slags, the prediction carries some level of confidence. Judging from the intervals between the lines of the five example slags, the increase in electrical conductivity accelerates with increasing $TiO_{2\ eq}$. A similar phenomenon is shown for high-FeO slags up to 100% FeO (Jiao and Themelis, 1988).

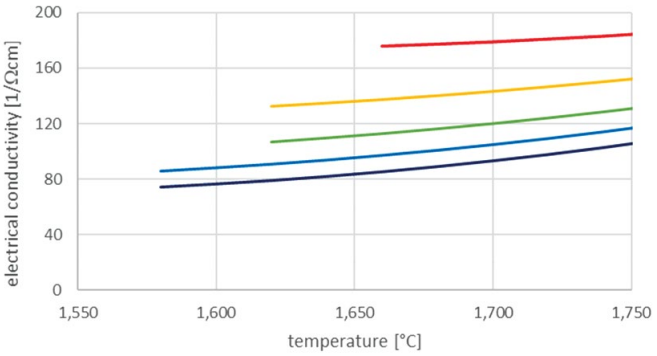


**Figure 10—Calculated electrical conductivities for the example slags (Table I), liquid state. The legend indicates %$TiO_{2\ eq.}$**

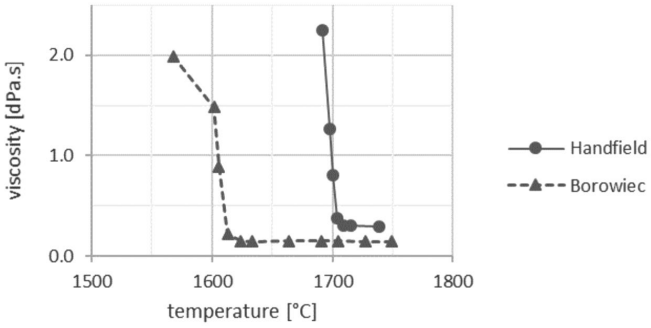


**Figure 11—Measured viscosities of $TiO_2$ slags reproduced from Handfield (Handfield and Charette, 1971) and Borowiec (Borowiec, 2009)**

## Viscosity

The viscosity of slags is known to be structure-dependent and high-$TiO_2$ slags are no different: above their liquidus temperatures $TiO_2$ slags dissociate into $Ti^{4+}$, $Ti^{3+}$, and $Fe^{2+}$; these have no structure such as $SiO_2$ networks provide for silicate slags. Consequently, fully liquid $TiO_2$ slags have very low viscosities. The measured data for 'low-FeO' Sorel slag (Handfield and Charette, 1971) and 95%QMM slag (Borowiec, 2009) are reproduced in Figure 11: above their liquidus temperatures these slags measured 0.3 dPa.s and 0.15 dPa.s. A recent study reports 0.6 dPa.s for fully liquid slags (Hu *et al.*, 2018). Though these numbers are different, they are all very low and not sensitive to composition or temperature. A second point of importance is that the critical temperature where viscosity increases sharply is only slightly below the slags' liquidus temperatures (Borowiec, 2009; Hu *et al.*, 2018).

Considering these results, the viscosities of the example slags (Table I) are estimated as shown in Figure 12. The dominant feature in these viscosity curves is the sharp upwards turn, the estimated positioning of which, was based on the calculated liquidus temperatures of the example slags given in Table II.

In industrial smelting the slag bath is likely to contain some unreacted reagent. The Einstein-Roscoe equation was used to quantify the impact thereof on the viscosity of the liquid bath (Equation [9]: viscosity of the liquid with solids, η [Pa.s]; viscosity of fully liquid phase η0 [Pa.s]; *f* volume fraction of the solids; assumed density for reductant 0.9 g/cm$^3$). This is an approximation because the Einstein-Roscoe equation was derived for solid spheres and reductants are often angular. The calculated

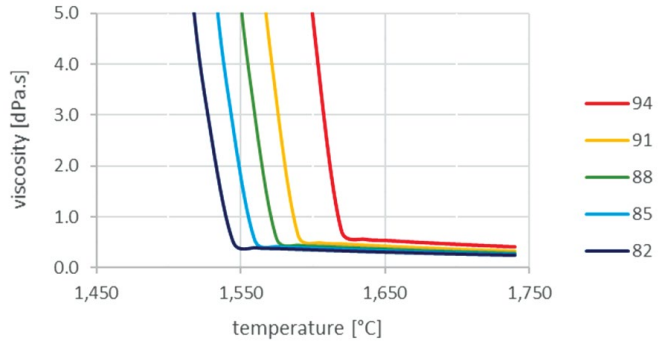


**Figure 12—Estimated viscosities for the example slags in Table I. The legend indicates %$TiO_2$**

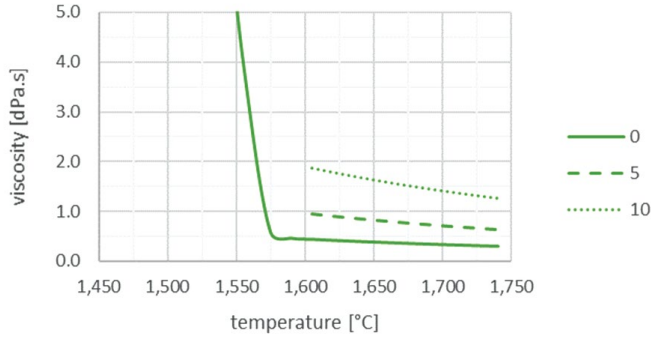


**Figure 13—Calculated viscosities for fully liquid slag (88%$TiO_2$) containing 0%, 5% and 10 mass% reductant**

viscosities for 0%, 5%, and 10mass% reductant in the 88%$TiO_2$ fully liquid slag are shown in Figure 13. At 10mass% reductant the viscosity of the slag bath increases from around 0.4 dPa.s to 1.5 dPa.s. This is similar to a change from olive oil at 35°C to maple syrup at 25°C (Nierat, Musameh, and Abdel-Raziq, 2014; Ngadi and Yu, 2004): not unmanageable – as Handfield points out: blast furnace slags are still tappable at 5 dPa.s, but also not insignificant considering the foaming tendency of $TiO_2$ slag baths.

$$\eta = \eta_0(1 - 1.35f)^{-2.5} \quad [9]$$

## Thermal conductivity

The thermal conductivity of solid $TiO_2$ slags was reported as 0.00175T + 0.3 W/m°C, which gives a thermal conductivity range of 1.0 to 2.9 W/m°C from 400°C to 1500°C (Kotze and Pistorius, 2010). Thermal conductivity measurements on solid $TiO_2$ slags from room temperature to 1050°C varied from just above 1 W/mK to approximately 2.5 W/mK with mostly, but not always, a positive relationship with temperature (Heimo, 2018). A single measurement in the same study gave 5 W/m°C at 1400°C. In the absence of data for liquid slag, 1 W/m°C is sometimes used in modelling (Zietsman and Pistorius, 2006). In the following paragraphs an attempt is made to approximate the thermal conductivity of high-$TiO_2$ slags based on the structure of these slags and their optical properties.

The thermal conductivity of slags is a combination of lattice $k_{latt}$, radiation $k_{rad}$, and electronic conduction $k_e$ (Mills and Susa, 1992). Lattice conduction is structure-dependent because it relies on the velocity of phonons $v$ through the slag, and the mean free path of phonons $L$ through the slag, (Equation [10]; heat capacity at constant pressure $C_p$). In solids the crystal lattice provides the structure along which phonons travel; in silicate slags, the $SiO_2$ network provides the means. Thermal conductivity values measured with the transient hot wire method, a technique which isolates lattice conductivity, range from 0.03 to 1 W/mK for silicate slags (Glaser and Sichen, 2013; Kang *et al.*, 2012). Lattice thermal conductivities decrease with increasing temperature, reflecting the diminishing slag structure with increasing temperature. In $TiO_2$ slags – judging from the low viscosities above liquidus temperatures – no significant structure exists. Lattice thermal conductivities in high-$TiO_2$ slags are therefore expected to be small. Nevertheless, the lattice conductivity where estimated from a correlation between reported transient hot wire thermal conductivities and calculated viscosities of silicate slags. The model used for viscosity calculations is based on the work by Zang (Zhang *et al.*, 2012, Zhang and Chou, 2012), a little-known model for $SiO_2$-$Al_2O_3$-CaO-MgO-FeO-MnO-$K_2O$ slags, but with good reproducibility of experimental data, and with potential to be expanded to more oxide components (Kotze, 2017).

$$k_{latt} = \frac{1}{3}C_p v L \quad [10]$$

The radiative component of thermal conductivity $k_{rad}$ is calculated with Equation [11] (Mills and Susa, 1992) (Stefan Boltzmann constant $\sigma = 5.67 \times 10^{-8}$ W/m$^2$K$^4$; refractive index of the slag $n$ [dimensionless]; temperature $T$ [K]; absorption coefficient $\beta$ [cm$^{-1}$] usually denoted as $\alpha$ in the literature but changed here to avoid confusion with the earlier mentioned electronic polarizability). The refractive indexes of the transition metal oxides are generally higher: 2 and more, compared to 1.535 for $SiO_2$, 1.805 for CaO, 1.715 for MgO, and 1.79 for $Al_2O_3$. Based on this the radiative component in the $TiO_2$ slags could be expected to be higher than for silicate slags. However, the absorption coefficient for FeO is two orders of a magnitude higher (Susa, Nagata, and Mills, 1993), and that of $Ti_2O_3$ three orders of a magnitude higher (Li, 2016) than those of $SiO_2$, CaO, MgO and $Al_2O_3$. Consequently, the radiative component of high-$TiO_2$ slags is low compared to low FeO silicate slags.

$$k_{rad} = \frac{16\sigma n^2 T^3}{3\beta} \quad [11]$$

The electronic thermal conductivity $k_e$ was calculated with the Wiedemann-Franz formula (Ok *et al.*, 2018) (Equation [12], electrical conductivity $\sigma$ [$\Omega^{-1}$m$^{-1}$]; Lorenz number $L = 2.44 \times 10^{-8}$ W$\Omega$/K$^2$; temperature T [K]). Due to the high electrical conductivity of $TiO_2$ slags, electronic conductivity, which is negligible in silicate slags, can be significant for $TiO_2$ slags.

$$k_e = \sigma L T \quad [12]$$

The etimated lattice, and calculated radiative and electronic conductivities of example slags 1, 3, and 5 (94%, 88%, and 82% $TiO_{2\ eq}$) are shown in Figure 14. Total thermal conductivities are shown with the thicker solid lines. The total thermal conductivity for liquid high-$TiO_2$ slags is estimated to range from 0.4 W/mK to close to 1 W/mK over the liquid temperature range. The thermal conductivity is predicted to increase non-linearly with increasing $TiO_{2\ eq}$ (Figure 15) which is attributed to the increase in electronic conduction with increasing $TiO_{2\ eq}$.

## Summary

Experimentally measured properties of high-$TiO_2$ slags were

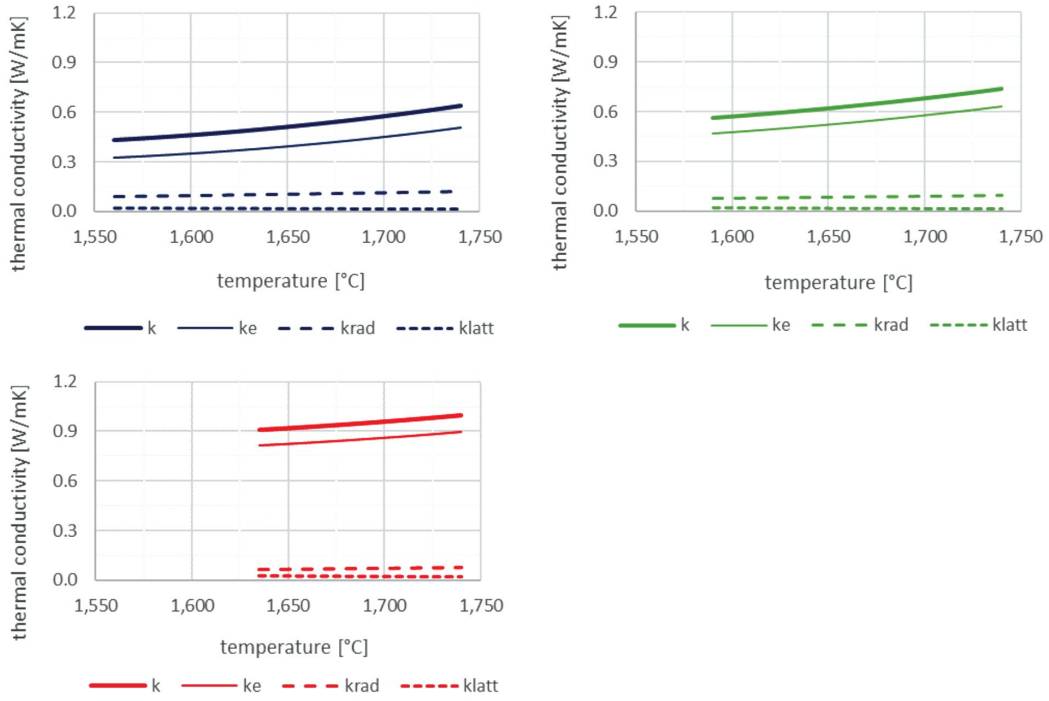


**Figure 14—Estimated total, lattice, radiative, and electronic thermal conductivity. Top left; 82% $TiO_{2\,eq}$; top right 88% $TiO_{2\,eq}$; bottom: 94%$TiO_{2\,eq.}$**

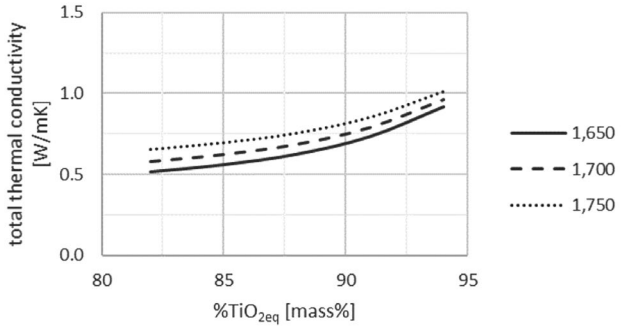


**Figure 15—Estimated total thermal conductivity for the example slags at 1650°C, 1700°C and 1750°C**

investigated and correlated with theoretically based parameters. Based on these correlations, the properties for five typical high-$TiO_2$ slags were calculated.

- The $Ti^{3+}/Ti^{4+}$ ratio of the liquid slags depends on the oxygen partial pressure and the oxygen activity in the bath. The polarizability ratio between $Ca^{2+}$ and $Si^{4+}$ cations was found to be a good parameter to quantify the oxygen activity. Future work will endeavor to investigate this concept against more $TiO_2$ slag data and other slag systems.
- Liquidus temperatures increase with decreasing FeO, but can increase or decrease with increasing $Ti_2O_3$ depending on the ratio between $Ti^{3+}$ and $Ti^{4+}$. Following on from the $Ti^{3+}/Ti^{4+}$ correlations, liquidus temperatures depend therefore on FeO, oxygen partial pressure, and the CaO and $SiO_2$ impurities. Other impurities such as MgO, MnO, $Al_2O_3$, $Cr_2O_3$, and $V_2O_5$ also affect liquidus values when they stabilize the $M_3O_5$ pseudobrookite phase. The partitioning of MnO between the $M_3O_5$ and silicate phases needs to be reviewed.
- The heat capacity of liquid high-$TiO_2$ slags cover a narrow range from 1000 to 1020 J/kgK.
- Liquid slag densities range from 3.5 to 3.7 g/cm³, with the lower range applying at higher temperatures and to higher $TiO_{2\,eq}$ slags.
- The electrical conductivities of liquid high-$TiO_2$ slags are one to two order of magnitudes higher than those of silicate slags and increase with increasing temperature. This is an important point for both AC and DC furnace design. The electrical conductivity of high-gangue $TiO_2$ slags correlates with the slags' electronic polarizability, while for low-gangue $TiO_2$ slags (high-$TiO_{2\,eq}$), the electrical conductivity was reproduced by using the slags' electronic polarizability and the valency ratio between Fe and Ti cations.
- The viscosities of high-$TiO_2$ slags above liquidus temperatures are very low but increase sharply just below liquidus temperatures. Though the viscosities of fully liquid slags are low, the presence of unreacted reductant in the bath will increase its viscosity.
- The thermal conductivities of liquid high-$TiO_2$ slags were derived from their viscosities and optical properties. For the example slags the thermal conductivities are estimated to range from 0.5 to 1 W/mK. Electronic thermal conduction is dominant and contributes to most to the total thermal conductivity.

Though the intention of this paper is to create a basis for extrapolation to $TiO_2$ slags not covered in the specific set of experimental work, the correlations derived here are still only applicable to the typical $TiO_2$, pseudobrookite $M_3O_5$ slags.

Slag properties are evasive: the need to estimate the thermal conductivity of the $TiO_2$ slags from theoretical considerations is a point in case. It is a complex field but our understanding of slag properties has expanded over the last approximate two decades. It is the author's hope that many a publication on the properties of $TiO_2$ slags is still to see the light.

## Acknowledgements

I would like to express sincere gratitude to all the researchers who contribute to the field of slag properties. My gratitude also goes to the referees who fulfilled their duty to challenge my thoughts and assumptions. And to all the designers and producers who apply this understanding of slag properties to optimize their processes: thank you for your support.

## References

Borowiec, K. 2009. *Partition of impurities within titania slag*. Santiago, Chile, s.n., pp. 23–31.

Brauer, G. and Littke, W. 1960. On the melting point and thermal dissociation of titanium dioxide. *Journal of Inorganic and Nuclear Chemistry*, vol. 16. pp. 67–76.

Desrosiers, R., Ajersch, F., and Grau, A. August 1980. *Electrical conductivity of industrial slags of high titania content*. Halifax, Nova Scotia, s.n.

Dimitrov, V. and Komatsu, T. 2010. An interpretation of optical properties of oxides and oxide glasses in terms of the electronic ion polarizability and average single bond strength. *Journal of the University of Chemical Technology and Metallurgy*, vol. 45, no. 3. pp. 219–250.

Dingwell, D.B. 1991. The density of titanium(IV) oxide liquid. *Journal of the American Ceramic Society*, vol. 74, no. 10. pp. 2718–2719.

Duffy, J. and Ingram, M. 1976. An interpretation of glass chemistry in terms of the optical basicity concept. J*ournal of Non-Crystalline Solids*, vol. 21, pp. 373–410.

Eriksson, G. and Pelton, A.D. 1993. Critical evaluation and optimization of the thermodynamic properties and phase diagrams of the MnO-$TiO_2$, MgO-$TiO_2$, FeO-$TiO_2$, $Ti_2O_3$-$TiO_2$, Na2O-$TiO_2$, and $K_2O$-$TiO_2$ systems. *Metallurgical Transactions B*, October, Volume 24B, pp. 795–805.

Eriksson, G. and Pelton, A.D. 1996. Measurement and thermodyamic evaluation of phase equilibria in the Fe-Ti-O system. *Ber. Bunsenges Phys Chem*, vol. 100, no. 11. pp. 1839–1849.

Frederikse, H. and Hosler, W. 1973. Electrical conductivity of coal slag. *Journal of the American Ceramic Society*, August, pp. 481–419.

Gaskell, D.R. 2008. *Introduction to the Thermodynamics of Materials*. Fifth edition ed. New York, London: Taylor & Francis.

Geldenhuis, J. and Pistorius, P. 1999. The use of commercial oxygen probes during the production of high titania slags. *Journal of the South African Institute of Mining and Metallurgy*, January/February, pp. 41–48.

Glaser, B. and Sichen, D. 2013. Thermal conductivity measurements of ladle slag using transient hot wire method. *Metallurgical and Materials Transactions B*, February, vol. 44B. pp. 1–4.

Handfield, G. and Charette, G. 1971. Viscosity and structure of industrial high-$TiO_2$ slags. *Canadian Metallurgical Quarterly*, vol. 10, no. 3. pp. 235–243.

Heimo, J. 2018. Thermal conductivity of titanium slags, Aalto: Aalto University.

Hu, K. *et al.*, 2018. Viscosity of $TiO_2$-FeO-$Ti_2O_3$-$SiO_2$-MgO-CaO-$Al_2O_3$ for high-titania slag smelting process. *Metallurgical and Materials Transactions B*, August, vol. 49B. pp. 1963–1973.

Ikemiya, N., Umemoto, J., Hara, S., and Ogino, K. 1993. Surface tension and densities of molten $Al_2O_3$, $Ti_2O_3$, $V_2O_5$ and $Nb_2O_5$. *ISIJ International*, vol. 33, no. 1. pp. 156–165.

Jiao, Q. and Themelis, N. 1988. Correlations of electrical conductivity to slag composition and temperature. *Metallurgical Transactions* B, February, vol. 19B. pp. 133–140.

Kang, Y. *et al.*, 2012. Thermal conductivity of the molten CaO-$SiO_2$-FeOx system. *Metallurgical and Materials Transactions B*, December, vol. 43B. pp. 1420–1426.

Kotze, H. 2017. *Comparison between viscosity models*, Consensi internal study.

Kotze, H. and Pistorius, P. 2010. A heat transfer model for high titania slag blocks. *Journal of the South African Institute of Mining and Metallurgy*, February, vol. 110. pp. 57–66.

Li, Y. 2016. *Investigation of titanium sesquioxide $Ti_2O_3$: synthesis and physical properties*, Thuwal, Kingdom of Saudi Arabia.

Mills, K. and Susa, M. 1992. *Thermal Conductivities of Slags*, Teddington, United Kingdom: National Physical Laboratory.

Ngadi, M. and Yu, L. 2004. Rgeological properties of Canadian maple syrup. *Canadian Biosystems Engineering*, vol. 46. pp. 3.15–3.18.

Nierat, T., Musameh, S., and Abdel-Raziq, I. 2014. Temperture-dependence of olive oil viscosity. *Materials Science An Indian Journal*, vol. 11, no. 7. pp. 233–238.

Ok, K.M. *et al.*, 2018. Effect of point and planar defects on thermal conductivity of $TiO_2$-x. *Journal of the American Ceramic Society*, vol. 101. pp. 334–346.

Pelton, A.D. and Blander, M. 1986. Thermodynamic analysis of ordered liquid solutions by a modified quiasochemical approach - application to silicate slags. *Metallurgical Transactions B*, December, vol. 17B. pp. 805–815.

Pesl, J. and Eric, R. 2002. High temperature carbothermic reduction of $Fe_2O_3$-$TiO_2$-$M_xO_y$ oxide mixtures. *Minerals Engineering*, vol. 15. pp. 971–984.

Pesl, J. and Eric, R.H. 1999. High-temperature phase relations and thermodynamics in the iorn-titanium-oxygen system. *Metallurgical and Materials Transactions B*, August, vol. 30B. pp. 695–705.

Pistorius, P. 2007. Ilmenite smelting: the basics. s.l. *The Southern African Institute of Mining and Metallurgy*, pp. 75–84.

Pistorius, P. C. 2002. The relationship between FeO and Ti2O3 in ilmenite smelter slags. *Scandanavian Journal of Metallurgy*, vol. 31. pp. 130–125.

Seim, S. 2011. Experimental investigations and phase relations in the liquid $FeTiO_3$-$Ti_2O_3$-$TiO_2$ slag system, Trondheim.

Seim, S. and Kolbensen, L. 2010. Update on the equilibrium between liquid Fe-Ti-O slags and metallic iron. *Steel Research International*, vol. 81, no. 12. pp. 1051–1055.

Shannon, R.D. and Fischer, R.X. 2016. Empirical electronic polarizabilities of ions for the prediction and interpretation of rerfactive indices: oxides and oxysalts. *American Mineralogist*, vol. 101, pp. 2288–2300.

Susa, M., Nagata, K., and Mills, K. 1993. Absorption coefficients and refractive indices of synthetic glassy slags containing transition metal oxides. *Ironmaking and Steelmaking*, vol. 20, no. 5. pp. 372–378.

Tranell, G., Ostrovski, O., and Jahanshahi, S. 1997. *The thermodynamics of titanium in CaO-MgO-$Al_2O_3$-$SiO_2$-$TiO_x$ slags*. Sydney, pp. 501–506.

Tranell, G., Ostrovski, O., and Jahanshahi, S. 2002. The equilibrium partitioning of titanium between $Ti^{3+}$ and $Ti^{4+}$ valency states in CaO-$SiO_2$-$TiO_x$ slags. *Metallurgical and Materials Transactions B*, February, vol. 33B. pp. 61–67.

Xin, J., Gan, L., Wang, N., and Chen, M. 2019. Accurate density calculation for molten slags in $SiO_2$-$Al_2O_3$-CaO-MgO-FeO-$Fe_2O_3$ systems. *Metallurgical and Materials Transactions B*, 50B(December). pp. 2828–2842.

Zhang, G.-H. and Chou, K.-C. 2012. Measuring and modeling viscosity of CaO-$Al_2O_3$-$SiO_2$(-$K_2O$) melt. *Metallurgical and Materials Transactions B*, August, vol. 43B. pp. 841–848.

Zhang, G.-H., Chou, K.-C., and Mills, K. 2012. Modelling viscosities of CaO-MgO-$Al_2O_3$-SiO2 molten slags. *ISIJ International*, vol. 52, no. 3. pp. 355–362.

Zhang, G.-H., Chou, K.-C., Xue, Q.-G., and Mills, K. C. 2012. Modeling viscosities of CaO-MgO-FeO-MnO-SiO2 molten slags. *Metallurgical and Materials Transactions B*, February, vol. 43B. pp. 64–72.

Zietsman, J. H. and Pistorius, P. 2006. Modelling of an ilmenite-smelting DC arc furnace process. *Minerals Engineering*, vol. 19. pp. 262–279. ◆